A Low-Voltage Actuated Micromachined Microwave Switch Using Torsion Springs and Leverage

Dooyoung Hah, Euisik Yoon, *Member, IEEE*, and Songcheol Hong, *Member, IEEE*

***Abstract*—In this paper, a push–pull type microwave switch is proposed, which utilizes torsion springs and leverage for low-voltage operation. The switching operation up to 4 GHz is demonstrated. The actuation voltage is ∼5 V. The insertion loss of ∼1 dB and the isolation as high as ∼40 dB at 1 GHz are achieved by the push–pull operation.**

***Index Terms*—Microactuators, micromachining, microwave switches.**

I. INTRODUCTION

MICROWAVE switches are widely used components in RF communication systems such as phase shifters, phased-array antenna, and handsets. Conventionally, semiconductor devices, such as FETs and p-i-n diodes, have been used for switch operation. However, they suffered from high-insertion loss and poor isolation. Since Larson *et al.*'s demonstration in the early 1990's, many researchers have reported micromachined switches [1]–[10]. From these switches, low-insertion loss and good isolation can be achieved compared to the semiconductor counterparts. Micromachined switches also have ultrahigh linearity.

Since most micromachined switches are operated by electrostatic actuation, their main drawback is the high actuation voltage (typically >20 V, minimum 8 V, as reported in [9]). This makes it difficult to be adapted for the miniaturized mobile systems. To reduce the actuation voltage, the gap between the movable contact and signal line should be reduced. However, this results in the increase of off capacitance (C_{off}), leading to poor isolation. The other approach is to optimize the geometrical sizes of the movable structure for low actuation voltage. However, this generally causes high residual stress. Another solution is to change the configuration of the structure. A push–pull configuration has been reported to significantly reduce the actuation voltage. In addition, this type of switch is more robust to the influence of environment such as vibration or physical impact because potential is applied at both on state and off state. Milanovic *et al.* demonstrated the switch of this configuration [10]. However, the maximum height of the movable contact is limited to the double of initial height in their scheme.

In this paper, we propose a new push–pull configuration by combination of rotational actuation and leverage for low-voltage actuation of the micromachined microwave switch. This paper will discuss the operation principle, design issues, fabrication techniques, experimental results, and areas requiring further research.

Manuscript received March 6, 2000; revised August 23, 2000. This work was supported in part under the National Research Laboratory Project and by the Millimeter-Wave Innovation Technology Research Center.

The authors are with the Department of Electrical Engineering and Computer Science, Korea Advanced Institute of Science and Technology, Taejon 305-338, Korea (e-mail: hady@cais.kaist.ac.kr).

Publisher Item Identifier S 0018-9480(00)10786-0.

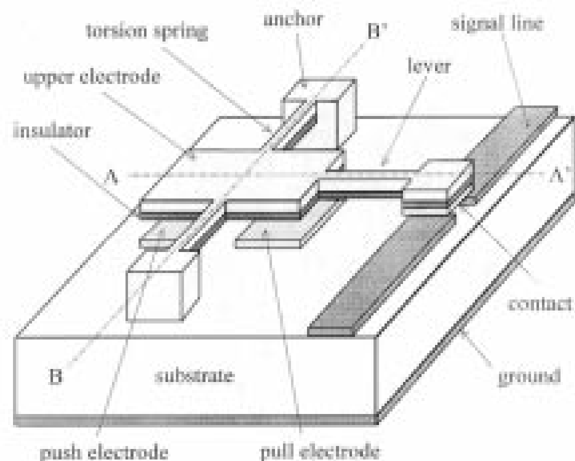

Fig. 1. Schematic diagram of the proposed switch.

II. PUSH–PULL CONFIGURATION

Fig. 1 shows the schematic diagram of the proposed switch. Microstrip transmission line has been used for our design. Initially, the signal line is separated and the switch is at the off state. When the contact arm is pulled down by electrostatic force, the contact is made in the signal line and signal can be transmitted at this on state. The isolation of the switch is determined by C_{off}. Since capacitance is inversely proportional to the distance between its two electrodes, the isolation becomes larger if the contact is lifted higher. For this purpose, we propose a push–pull configuration. The contact is suspended to a lever physically and isolated with it electrically by insulator. The lever is connected to a rotational plate, which rotates around an axis of torsion springs. One end of the torsion spring is anchored to the substrate. There are two fixed electrodes on the substrate. One is a push electrode and the other is a pull electrode. When voltage is applied to the pull electrode, as shown in Fig. 2(b), the contact moves down to make contact with the signal line. When this pull voltage is eliminated and the push voltage is applied, as shown in Fig. 2(c), the contact is lifted upward. The contact height (h_c) at the off state is amplified by the leverage. The contact height (h_c) is expressed as [see Fig. 2(a)]

$$h_c = \left(2 + \frac{l_{\text{lever}}}{l_{\text{te}}}\right) h_0 \tag{1}$$

0018–9480/00$10.00 © 2000 IEEE

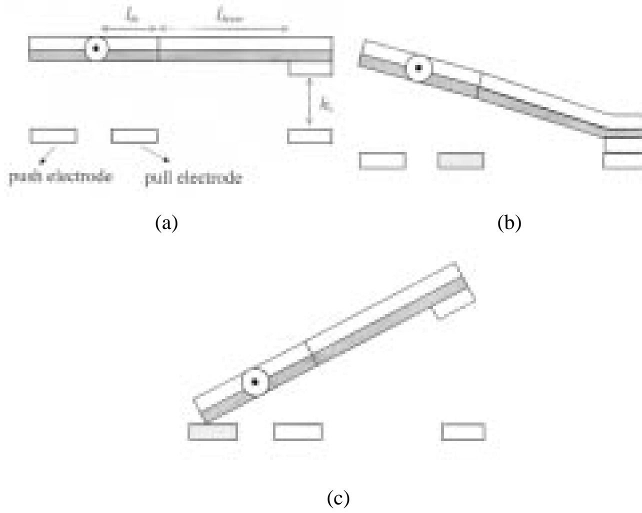

Fig. 2. The proposed push–pull configuration. (a) At zero bias. (b) At the on state (when $V_{\rm pull}$ is on). (c) At the off state (when $V_{\rm push}$ is on).

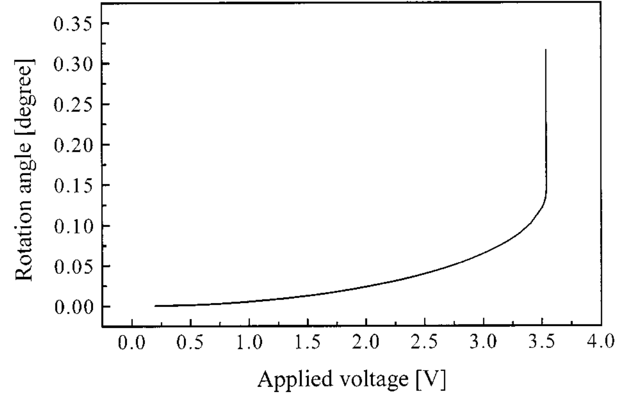

Fig. 3. Calculated rotation angle versus the applied voltage.

where h_0 is the initial height. It shows that h_c (hence, isolation) increases as $l_{\rm lever}$ increases. Therefore, we can make h_0 lower to reduce the actuation voltage while maintaining high isolation.

A. Electrostatic Torque and Actuation Voltage

Since the switching is carried out by the electrostatic torque, one has to know the relation between electrostatic torque (T_e) and rotation angle (θ) to estimate the actuation voltage, i.e.,

$$T_e(\theta) = \frac{\varepsilon_0 V^2 w_{\rm te}}{2\sin^2\theta}\left[\frac{l_{\rm te}\sin\theta}{h_0 - l_{\rm te}\sin\theta + t_d/\varepsilon_d} + \ln(h_0 - l_{\rm te}\sin\theta + t_d/\varepsilon_d) - \frac{l_e\sin\theta}{h_0 - l_e\sin\theta + t_d/\varepsilon_d} - \ln(h_0 - l_e\sin\theta + t_d/\varepsilon_d)\right] \tag{2}$$

where V is an applied voltage, $w_{\rm te}$ is the width of the upper electrode, l_e is $(l_{\rm te} - l_{\rm be})$, and $l_{\rm be}$ is the length of the bottom electrode, and t_d and ε_d are the thickness and dielectric constant of the insulator, respectively. At equilibrium, T_e is equal to the restoring torque (T_r), which can be written as

$$T_r(\theta) = \frac{2GJ\theta}{l_s} \tag{3}$$

where l_s is the length of the torsion spring and G is the shear modulus. J is the polar moment of inertia of the spring, which is expressed as

$$J = \frac{w_s t_s}{12}\left(w_s^2 + t_s^2\right) \tag{4}$$

where w_s and t_s are the width and the thickness of the spring, respectively. One can obtain the relation between θ and the applied voltage by solving the equation

$$T_e(\theta) = T_r(\theta). \tag{5}$$

When V is small, there exists a solution. However, above a threshold voltage ($V_{\rm th}$), (5) cannot be solved. This means that the upper electrode is abruptly pulled down to touch the bottom electrode at $V_{\rm th}$. Fig. 3 shows the calculated relation between applied voltage and rotation angle. In this case, $V_{\rm th}$ is 3.5 V. The off voltage ($V_{\rm push}$) is $V_{\rm th}$ because the upper electrode directly touches the push electrode. The on voltage ($V_{\rm pull}$) can be lower than $V_{\rm th}$ because the contact can be touched to the signal line before the upper electrode is to the pull electrode. Therefore, the overall actuation voltage of the switch is estimated to be about $V_{\rm th}$.

III. Design

In order to design the micromachined microwave switch, the switching voltage and RF performance must be primarily considered. To achieve low actuation voltage, the geometrical dimensions of the actuation part have to be optimized. To have good RF performance, contact part needs to be carefully designed.

A. Actuation Part

Fig. 4 shows the calculated $V_{\rm th}$ with various geometrical dimensions. It is found in Fig. 4(a) that $V_{\rm th}$ is dependent more on the spring width (w_s) than on the spring length (l_s). Fig. 4(b) shows that the gap between the upper and bottom electrodes (h_0) is more influential than the thickness of the torsion spring (t_s) to achieve the low actuation voltage. Without using a push–pull configuration, the maximum contact height (h_c) at the off state is the same as the initial height (h_0). In this case, h_0 must be high enough for reasonable RF isolation. Then, $V_{\rm th}$ is ~30 V when t_s is 2 μm and h_0 is 4 μm. The push–pull configuration allows that h_0 can be lowered by the half while maintaining the same isolation. In this case, $V_{\rm th}$ is decreased to 10 V (about one-third of the non-push–pull type ones). By combination of the rotational actuation and the leverage, we can lower h_0 further with the same isolation. When $l_{\rm lever}$ is $2l_{\rm te}$ and h_0 is 1 μm, $V_{\rm th}$ is decreased to 3.5 V (about one-third of that without leverage). Fig. 4(c) shows that $V_{\rm th}$ decreases as the upper electrode length $(l_{\rm te})$ and the width $(w_{\rm te})$ increase. This also shows that $V_{\rm th}$ is not decreased significantly when the ratio of $l_{\rm be}/l_{\rm te}$ is greater

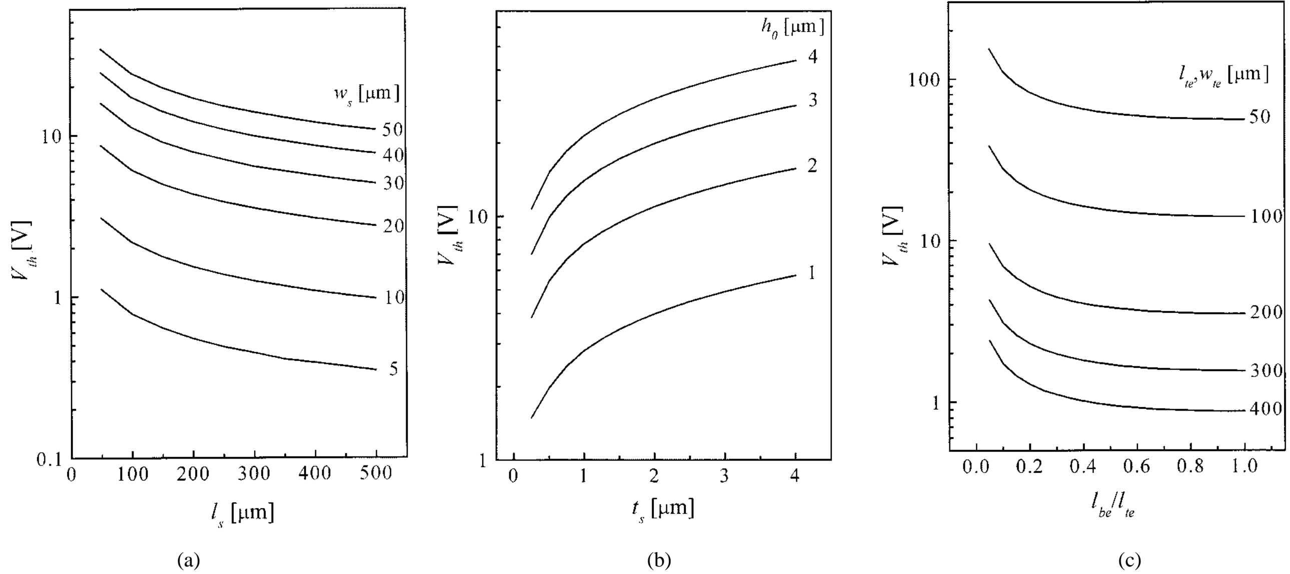

Fig. 4. Calculated $V_{\rm th}$ of the switch: (a) with various spring widths (w_s) and spring length (l_s), (b) with various initial contact heights (h_0) and spring thickness (t_s), and (c) with various bottom ($l_{\rm bc}$) and upper electrode length ($l_{\rm tc}$).

TABLE I
DESIGNED DIMENSIONS OF THE MICROMACHINED SWITCH

Parameter	value
spring width (w_s)	20
spring length (l_s)	300
upper electrode width (w_{te})	100 to 400
upper electrode length (l_{te})	100 to 400
bottom electrode length (l_{be})	$0.8l_{te}$
lever width (w_{lever})	50
lever length (l_{lever})	l_{te} to $3l_{te}$

than 0.4. The dimensions of the fabricated switch are shown in Table I.

B. Contact Part

The RF model of the switch at the on and off states is depicted in Fig. 5(a) and (b), respectively. C_p is the parasitic capacitance between the contact electrode and upper electrode. The off state is modeled as the parallel connection of the vertically coupling capacitance (C_V) and the microstrip gap ($M_{\rm GAP}$). Fig. 6(a) shows the calculated insertion loss with various on resistance ($R_{\rm on}$) and C_ps at 4 GHz. When $R_{\rm on}$ is greater than 5 Ω, $R_{\rm on}$ becomes the dominant factor, and when $R_{\rm on}$ is less than 5 Ω, the insertion loss is mainly determined by C_p. Fig. 6(b) shows the calculated isolation with various C_Vs and the signal line gap (s) at 4 GHz. When C_V is greater than 50 fF, the isolation is determined by C_V. Smaller than 50 fF, s begins to affect the isolation. The contact area has to be designed carefully to have good RF performance. As the contact area increases, $R_{\rm on}$ decreases and $C_{\rm off}$ increases. The designed contact area is 90 × 90 μm^2.

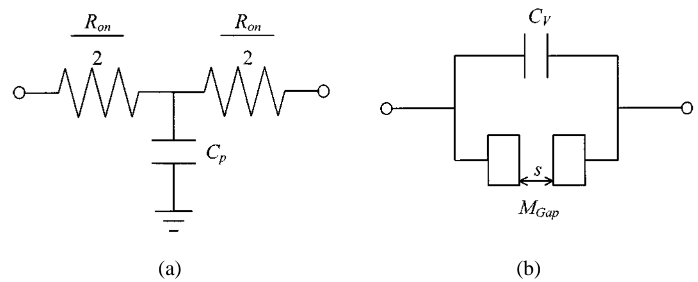

Fig. 5. RF models of the micromachined switch. (a) At the on state. (b) At the off state.

C. Stress Management

Control of stress is very important in the design of the switch. When the overall structure has a tensile stress (bent downward), isolation becomes poor. When it has a compressive stress (bent upward), the contact cannot be formed in the pull operation. Plated Au is selected as a main structural layer due to its small shear modulus and moderate stress. The whole movable structure is designed as a multilayer of SiN_x (200 nm)—evaporated Ti/Au (20/50 nm)—plated Au (1.1 μm) as a stress compensated structure. SiN_x with a compressive stress is inserted to compensate the moderate tensile stress gradient of the electroplated Au. It also works as an insulating layer between the dc bias and the contact. It prevents short between the upper and bottom electrodes. Total thickness of the movable structure is 1.4 μm.

IV. FABRICATION

In this study, semiinsulating GaAs has been used as the substrate. Other insulating or semiinsulating substrates, such as high-resistivity Si, alumina, quartz, etc., can also be used. Fig. 7 shows the fabrication process. At first, the signal line and the bottom (push and pull) electrodes are formed by Au plating on top of the Ti/Au seed metal. After removal of the seed metal [see Fig. 7(a)], AZ5214 photoresist is spun as a

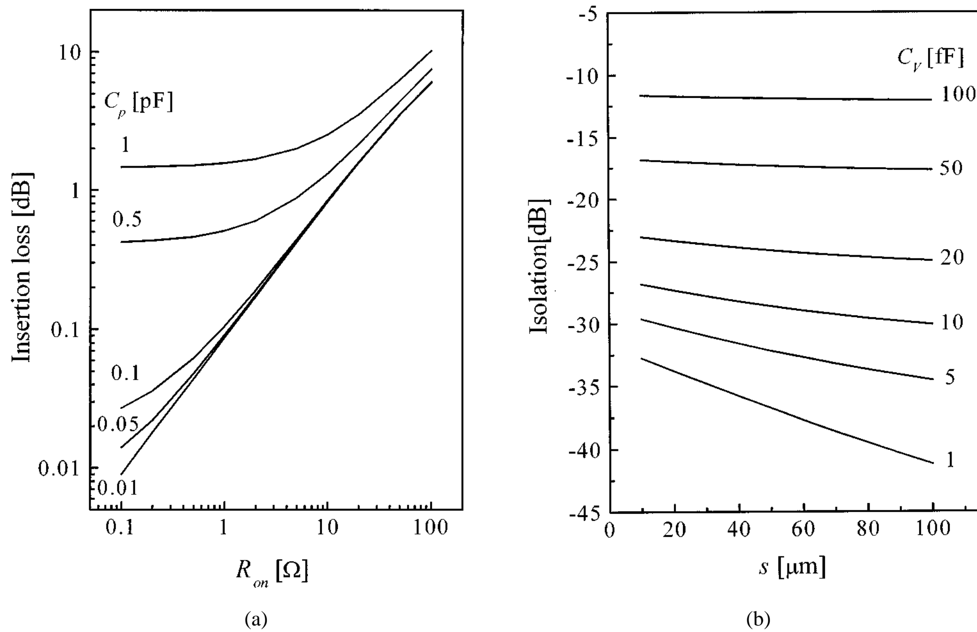

Fig. 6. Calculated RF characteristics of the switch. (a) At the on state. (b) At the off state.

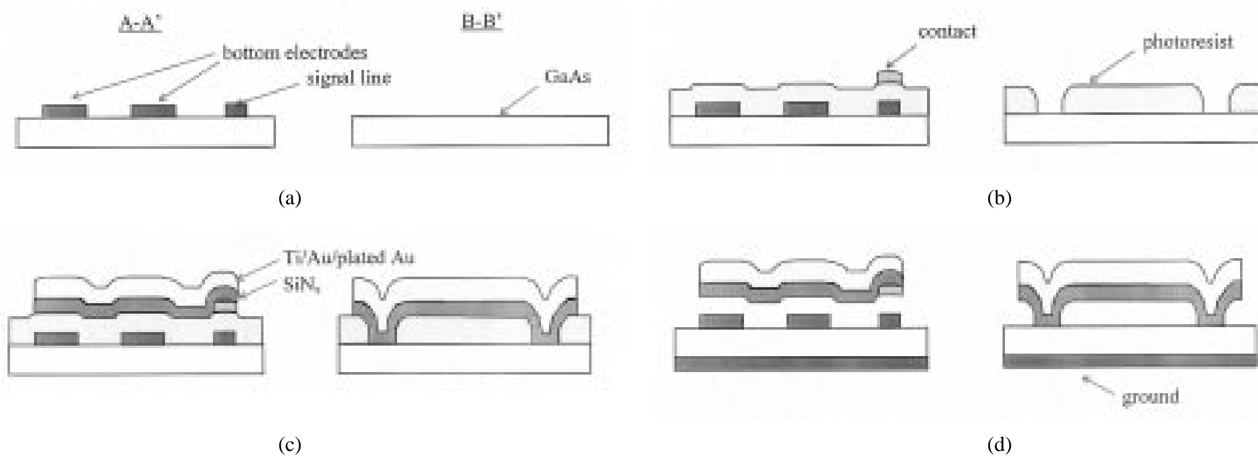

Fig. 7. Fabrication process of the switch. (a) Formation of the bottom electrodes and signal line. (b) Sacrificial layer and contact formation. (c) Structure layer formation. (d) Structure release.

sacrificial layer and anchor is defined. The photoresist is cured at 150 °C to endure during the next process steps. The contact is formed by Au/Ti (0.5/0.05 μm) evaporation and wet etching [see Fig. 7(b)]. Au is selected because of its high conductivity and antioxidation property. Ti is inserted for the adhesion of Au and SiN_x. After formation of the total movable structure described in the previous section [see Fig. 7(c)], the ground plane (Au) is plated at the backside and the structure is released [see Fig. 7(d)]. This release step is performed by O_2 plasma dry etching to prevent the stiction problem. The SEM micrograph of the fabricated switch is shown in Fig. 8. The contact is floated 1 μm above the signal line.

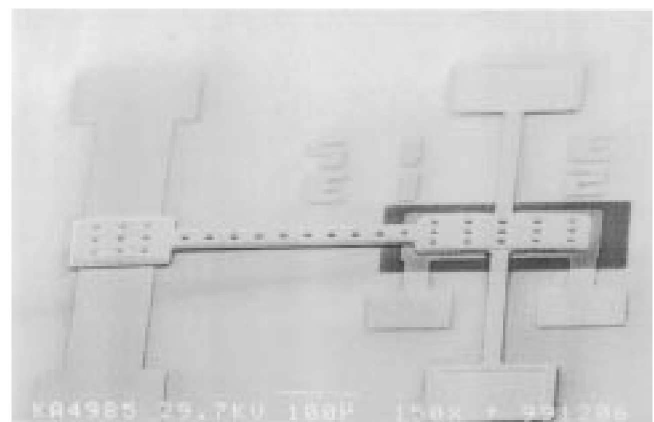

Fig. 8. SEM micrograph of the fabricated switch.

V. RESULTS

Fig. 9 shows the C–V measurement result between the upper and bottom electrodes of the fabricated switch. It shows that the capacitance is abruptly changed at 4 V. Fig. 10 shows the measured $V_{\rm pull}$ and $V_{\rm push}$ of the switch with various $l_{\rm te}$s. It shows

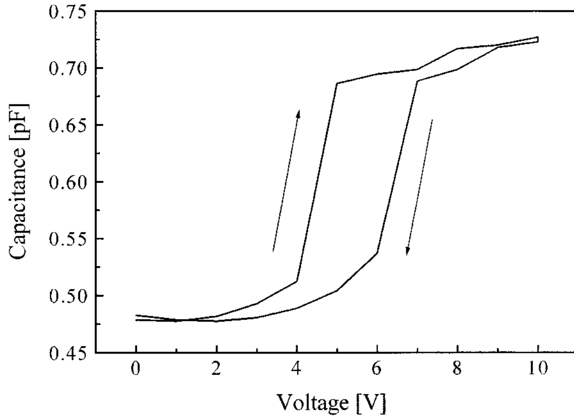

Fig. 9. C–V measurement result of the fabricated switch.

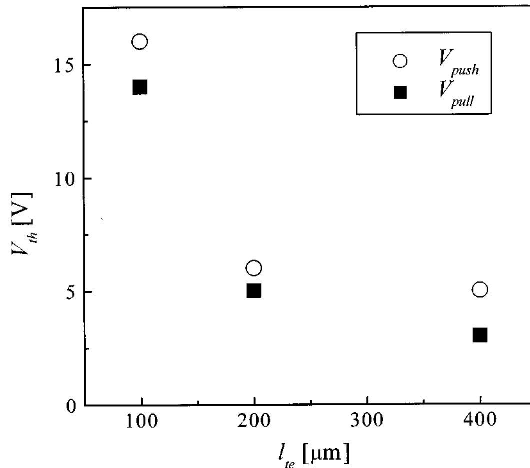

Fig. 10. Measured $V_{\rm pull}$ (square) and $V_{\rm push}$ (circle) of the switch with various $l_{\rm tc}$s.

that $V_{\rm pull}$ is lower than $V_{\rm push}$. $V_{\rm pull}$ is 3–14 V and $V_{\rm push}$ is 5–16 V. These low actuation voltages are due to the small initial gap (1 μm) between the upper and bottom electrodes. The dynamic response of the switch at 100 Hz is given in Fig. 11. In a non-push–pull configuration, the closure and release times were measured as 0.5 and 0.1 ms, respectively. In the push–pull configuration, both of the times are 0.6 ms. The RF characteristics from 500 MHz to 4 GHz of the fabricated switch have been examined by using the HP8720C network analyzer. Fig. 12 shows the on state characteristics of the switch. $R_{\rm on}$ and C_p are extracted as 10 Ω and 0.6 pF. The reason for this high $R_{\rm on}$ may be that hard contact is not formed because of the distance between the pull electrode and contact electrode. The insertion loss is lower than 2 dB. To achieve the insertion loss as low as 0.1 dB at 4 GHz, $R_{\rm on}$ must be below 1 Ω and C_p below 50 fF. The off-state characteristics of the fabricated switch are shown in Fig. 13. When no bias is applied, the isolation has been measured as >17 dB. It becomes >28 dB in the push operation, improving the isolation by ~10 dB. C_V have been estimated as 60 fF at zero bias and considerably reduced to 6 fF by the push operation. Total $C_{\rm off}$ has been calculated to be 70 fF at zero bias and 15 fF by the push operation. The signal line gap (s) was

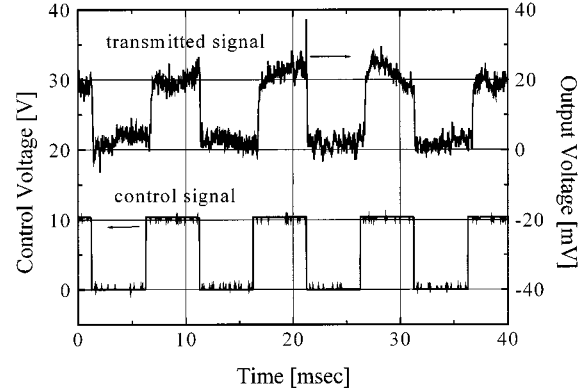

Fig. 11. Dynamic response of the switch.

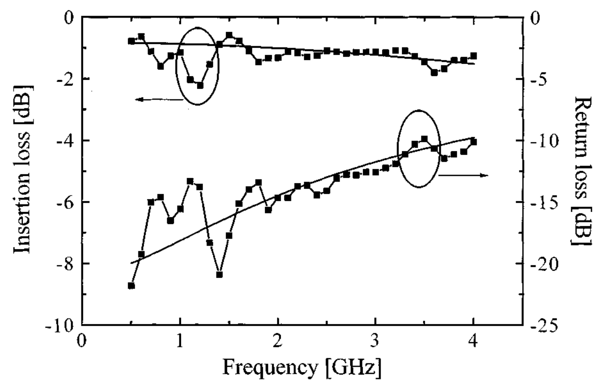

Fig. 12. Measured (line + symbol) and modeled (line) on state characteristics of the fabricated switch.

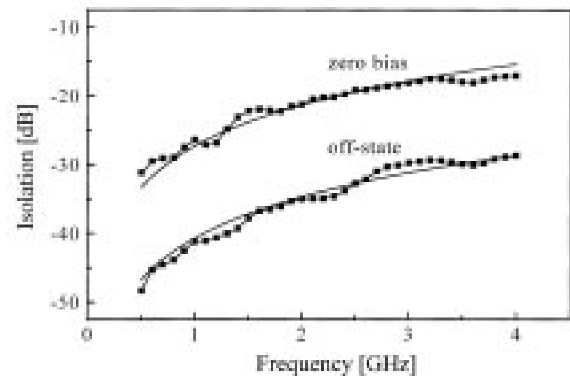

Fig. 13. Measured (line + symbol) and modeled (line) off state characteristics of the fabricated switch.

20 μm. With the wider gap, the isolation becomes greater. The lifetime of the switch is under estimation.

VI. Conclusions

A surface-micromachined microwave switch with a push–pull configuration has been proposed and demonstrated in this paper. A low actuation voltage has been achieved by means of torsion springs and leverage. DC measurements have indicated that the minimum actuation voltage is lower than 5 V. RF characterizations show that the isolation can be significantly

improved by the push–pull configuration. This switch can be used for mobile RF telecommunication systems.

ACKNOWLEDGMENT

The authors would like to thank D. Baek, Korea Advanced Institute of Science and Technology (KAIST), Taejon, Korea, M. Kim, KAIST, Taejon, Korea, E. Park, KAIST, Taejon, Korea, and Y. Kang, KAIST, Taejon, Korea, for their fabrication aid.

REFERENCES

[1] L. E. Larson, R. H. Hackett, M. A. Melendes, and R. F. Lohr, "Micromachined microwave actuator (MIMAC) technology—A new tuning approach for microwave integrated circuits," in *IEEE Microwave Millimeter-Wave Monolithic Circuit Symp. Dig.*, Boston, MA, June 10–11, 1991, pp. 27–30.

[2] J. J. Yao and M. F. Chang, "A surface micromachined miniature switch for telecommunications applications with signal frequencies from DC up to 4 GHz," in *8th Int. Solid-State Sens. Actuators Eurosens. Conf.* , Stockholm, Sweden, June 25–29, 1995, pp. 384–387.

[3] C. Goldsmith, J. Randall, S. Eshelman, and T. H. Lin, "Characteristics of micromachined switches at microwave frequencies," in *IEEE MTT-S Int. Microwave Symp. Dig.*, San Francisco, CA, June 18–20, 1996, pp. 1141–1144.

[4] S. Pacheco, C. T. Nguyen, and L. P. B. Katehi, "Micromechanical electrostatic K-band switches," in *IEEE MTT-S Int. Microwave Symp. Dig.*, Baltimore, MD, June 9–11, 1998, pp. 1569–1572.

[5] C. Goldsmith, Z. Yao, S. Eshelman, and D. Denniston, "Performance of low-loss RF MEMS capacitive switches," *IEEE Microwave Guided Wave Lett.*, vol. 8, pp. 269–271, Aug. 1998.

[6] D. Hyman, A. Schmitz, B. Warneke, T. Y. Hsu, J. Lam, J. Brown, J. Schaffner, A. Walston, R. Y. Loo, G. L. Tangonan, M. Mehregany, and J. Lee, "GaAs-compatible surface-micromachined RF MEMS switches," *Electron. Lett.*, vol. 35, pp. 224–226, Feb. 1999.

[7] J. B. Muldavin and G. M. Rebeiz, "30 GHz tuned MEMS switches," in *IEEE MTT-S Int. Microwave Symp. Dig.*, Anaheim, CA, June 14–17, 1999, pp. 1511–1514.

[8] K. Suzuki, S. Chen, T. Marumoto, Y. Ara, and R. Iwata, "A micromachined RF microswitch applicable to phased-array antennas," in *IEEE MTT-S Int. Microwave Symp. Dig.*, Anaheim, CA, June 14–17, 1999, pp. 1923–1926.

[9] J. Park, G. Kim, K. Chung, and J. Bu, "Electroplated RF MEMS capacitive switches," in *13th Int. IEEE MEMS Conf. Tech. Dig.*, Miyazaki, Japan, Jan. 23–27, 2000, pp. 639–644.

[10] V. Milanovic, M. Maharbiz, A. Singh, B. Warneke, N. Zhou, H. K. Chan, and K. S. J. Pister, "Microrelays for batch transfer integration in RF systems," in *13th Int. IEEE MEMS Conf. Tech. Dig.*, Miyazaki, Japan, Jan. 23–27, 2000, pp. 787–792.

Dooyoung Hah was born in Seoul, Korea, in 1972. He received the M.S. and Ph.D. degrees in electrical engineering from the Korea Advanced Institute of Science and Technology (KAIST), Taejon, Korea, in 1996 and 2000, respectively.

His research interests are in optomechanical microsensors and micromachined microwave integrated circuits.

Euisik Yoon (S'80–M'82) was born in Seoul, Korea. He received the B.S. and M.S. degrees in electronics engineering from Seoul National University, Seoul, Korea, in 1982 and 1984, respectively, and the Ph.D. degree in electrical engineering from The University of Michigan at Ann Arbor, in 1990.

From 1990 to 1994, he was with the Fairchild Research Center, National Semiconductor Corporation, Santa Clara, CA, where he was engaged in researches on deep submicrometer CMOS integration and advanced gate dielectrics. In 1996, he joined the Department of Electrical Engineering, Korea Advanced Institute of Science and Technology (KAIST), Taejon, Korea, where he is currently an Assistant Professor. He also currently serves as a Technical Advisory Board Member for Sandcraft Inc., Santa Clara, CA. His current research interests are in microsensors, integrated microsystem, and very large scale integration (VLSI) circuit design.

Songcheol Hong (S'87–M'88) was born in Korea, in 1959. He received the B.S. and M.S. degrees in electronics from the Seoul National University, Seoul, Korea, in 1982 and 1984, respectively, and the Ph.D. degree in electrical engineering from The University of Michigan at Ann Arbor, in 1989.

He is currently a Professor in the Department of Electrical Engineering, Korea Advanced Institute of Science and Technology (KAIST), Taejon, Korea. His research interests include optoelectronic integrated circuits, quantum-effect devices, and monolithic microwave integrated circuits (MMICs).